Supramolecular coordination chemistry

Leroy Cronin
DOI: 10.1039/b514843j

Highlights include the formation of ultra-large macrocycles with over 200 non-hundred atoms within a given cycle. The realisation that single molecule magnetic behaviour is not limited to molecules with high spin states. The connection of S = 1/2 cluster rings using a fragment that can switch on magnetic exchange between the clusters is extremely interesting for the synthesis of QBITs and electronically switchable units spatially well organised have been identified as providing routes to designing quantum cellular automata. The isolation of a fundamentally new DNA-small molecule binding mode *via* a three-way-junction has also been discovered. A stable chiral polyoxometalate has been found as well as a POM fragment that appears to stabilize a Pt═O moiety as well as a new Dawson-type structure that undergoes a coupled unprecedented structural and electronic reorganisation.

1. Introduction and scope

This report focuses on the development in the design, synthesis, self-assembly of metal-based architectures and ligands designed to aid in the construction of metallo-supramolecular architectures. The pace at which modern crystallographic analysis using area detectors is accelerating the discovery of new clusters, supramolecular architectures *etc*. continues to grow at a seemingly near exponential rate. The degree of selectivity applied when compiling this account is, therefore, high. Many crystal structures have been included in this report to aid visualisation and conceptualisation of the many interesting metallo-supramolecular architectures that have been constructed. A common colour scheme/size scheme is used in all the structural figures unless otherwise stated; the carbon atoms are light grey, nitrogen atoms white, metal ions large black spheres, sulfur atoms large grey spheres, oxygen or phosphorus atoms are small black spheres.

2. Metallomacrocycles, grids and wheels

Triangular $\{Dy_3\}$ clusters of the form, $[Dy_3(\mu_3\text{-}OH)_2L^1{}_3Cl_x(H_2O)_y]^{n+}$ ($x = 2$, $y = 4$; $x = 1$, $y = 5$ where $n = 4 - x$) have been discovered from the complexation of *o*-Vanillin (HL^1). This ligand has a tridentate chelating ligand bridging two Dy centres. Each of the Dy^{III} ions comprising the triangular cluster is bridged by two μ_3 hydroxide groups, each bridging one face of either side of the triangle. Importantly the compound shows a vanishing magnetic susceptibility at low temperature, and in spite of the almost non-magnetic ground state, features typical of a single molecule magnet are seen. This is important since the presence of a large spin ground state does not appear to be required for SMM-like behaviour.[1]

Department of Chemistry, The University of Glasgow, University Avenue, Glasgow, UK G12 8QQ

The complexation L^2 with the long linker $[Pd(NO_3)_2](L^3)$ allows an ultramacrocyclization through reversible catenation, see Fig. 1. The Pd^{II} clipped macrocycle shown in Fig. 1 has a nanometer-sized framework and easily forms the catenated dimer in polar media through p–p aromatic interactions between the two rings. In expectation of ultramacrocyclization through catenation, it was designed so that the long acyclic compound $[(PdL^2)_2L^3]$ (Pd_2), which comprises the Pd^{II} clipped macrocyclic units at both ends, in which the (Pd_2) units can selectively catenate into the ultramacrocyclic dimer (Pd_4), containing over 200 non-hydrogen atoms in its backbone.[2]

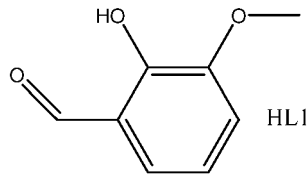

HL1

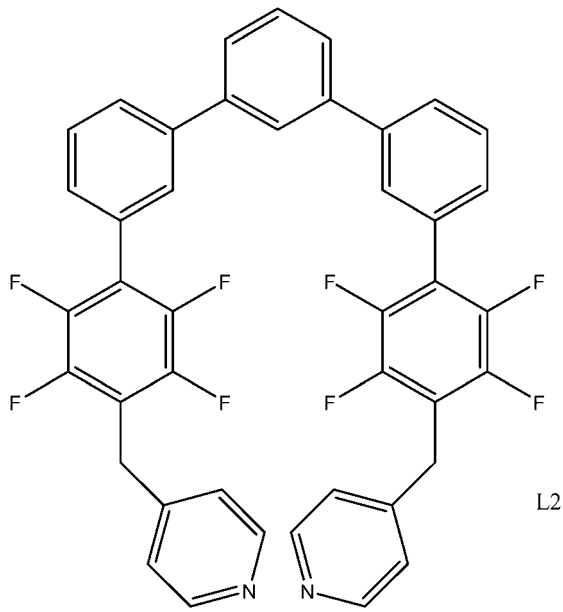

L2

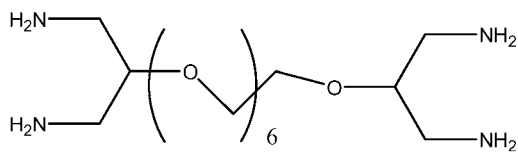

L3

The self assembly of neutral platinum-based supramolecular ensembles incorporating oxocarbon dianions and oxalate has been achieved. Five neutral platinum-based [2 + 2] macrocycles incorporating cyclic oxocarbondianions, squarate and croconate and their acyclic analogue, oxalate, have been synthesized in 90–95% yield *via* self-assembly. The combination of the diplatinum molecular clip (L^4Pt_2) with all three dianions afforded molecular rectangles, whereas a platinum-based 60° acceptor unit

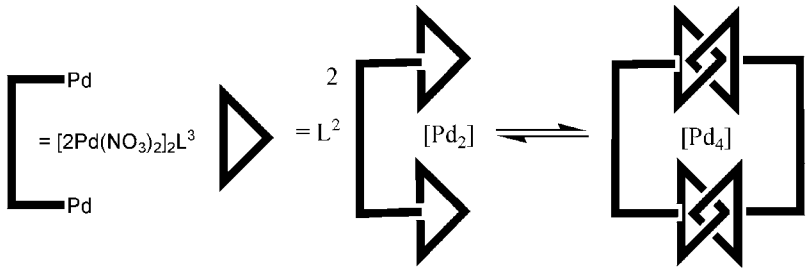

Fig. 1 A cartoon showing the formation of (Pd_2) and the selective catenation to (Pd_4).

(L^5Pt_2) produced a supramolecular triangle with three bridging squarate ions. In all cases, multinuclear NMR spectra were consistent with the formation of single highly symmetrical species. Thus, the self assembled platinum(II)-based complexes are characterised as neutral and finite supramolecular macrocycles incorporating interesting functional oxocarbon dianions [$(L^7)^{2-}$ and $(L^8)^{2-}$] and the oxalate moiety $(L^6)^{2-}$] see Fig. 2. The main difference between the dicarboxylates and oxocarbon-dianions is that the two carboxylate groups of the former are oriented in a definite direction and they act as rigid linkers to form assemblies of predetermined shape and size. Further, the assembly of these macrocycles gives an insight into the importance of entropy in controlling the size of the self-assembled species.[3] Also, coordination-driven self assemblies with a carborane backbone comprising a rectangle, triangle, a hexagon and squares have been designed that incorporate carborane building blocks.[4]

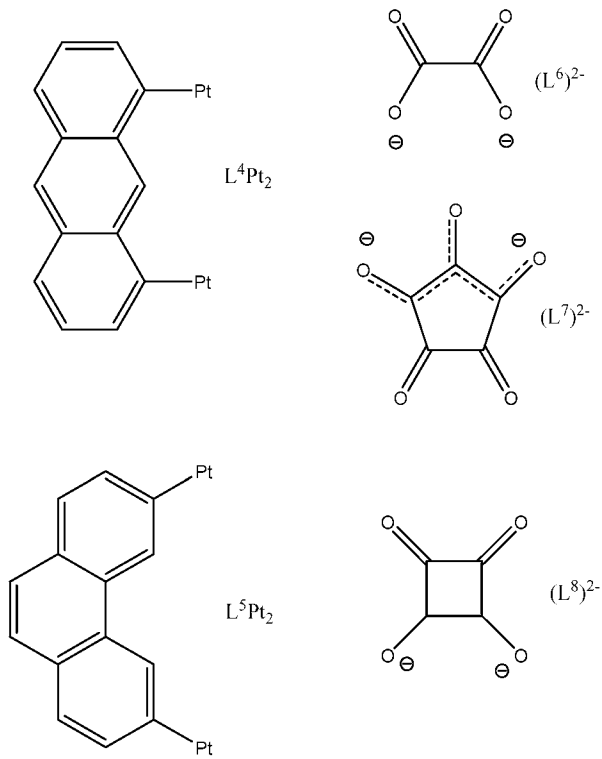

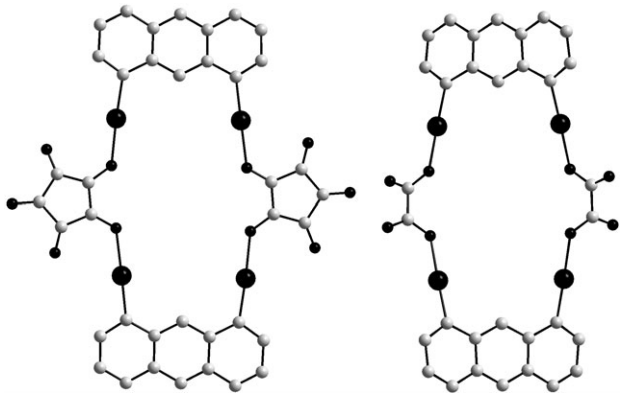

Fig. 2 Representations of the structures of $[(L^4Pt_2)_2(L^7)_2]$ (LHS) and $[(L^4Pt_2)_2(L^6)_2]$ (RHS).

Metal templated diyne cyclodimerisation and cyclotrimerisation was achieved using the phosphine-substituted diyne bis-(diphenylphosphino)butadiyne, ($Ph_2PC_4PPh_2$), which are templated by coordination of the diyne to platinum *via* phosphorus. Reaction with $[Pt(CH_3)_2(COD)]$ led to a mixture of the bridged dimer $[\{Pt(CH_3)_2\}_2(\mu\text{-}Ph_2PC_4PPh_2)_2]$ and the trimer $[\{Pt(CH_3)_2\}_3(\mu\text{-}Ph_2PC_4PPh_2)_3]$ in an 85:15 ratio. It was found that the ratio is insensitive to concentration and temperature. The first compound consists of two *cis* square planar platinum centres bridged by two bisphosphino diyne units. The two square planes are close to perpendicular (*ca.* 86.1°) as a result of a twist in the overall geometry of the complex, which is necessary to accommodate the square planar geometry at platinum and the tetrahedral geometry at phosphorus. This geometry results in a close approach of the alkyne units on adjacent phosphines, with center-to-center distances of 3.34 and 3.27 Å. The carbon-carbon distances within the alkyne chain clearly indicate localized bonding, with alternating long and short distances.[5]

A cyanide bridge ring has been discovered incorporating 12 metal centres of the form: $[Mn^{III}(L^9)]_6[Fe^{III}(L^{10})(CN)_2]_6$ (H_2L^9 = *N*,*N*′-ethylenebis(salicylideneamine), H_2L^{10} = 1,2-bis(pyridine-2-carboxamido)-4-methylbenzene).[6] This is the largest cyanide-bridged heterometallic metallamacrocycle to date and is especially interesting due to its nanosized cavity, see Fig. 3, and because magnetic measurements

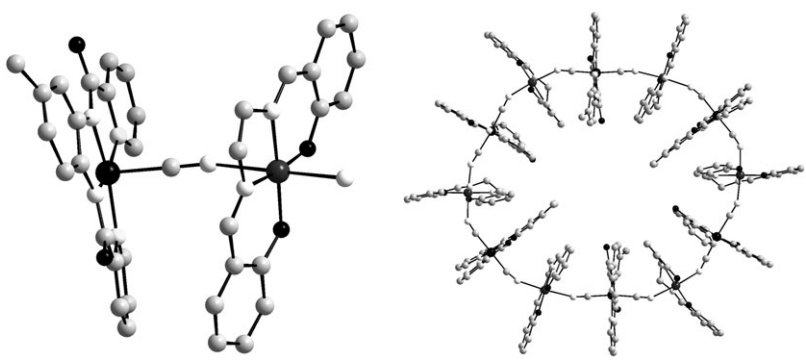

Fig. 3 Structure of the $[Mn^{III}(L^9)]_6[Fe^{III}(L^{10})(CN)_2]_6$ (top view RHS), segment showing both ligand types (LHS).

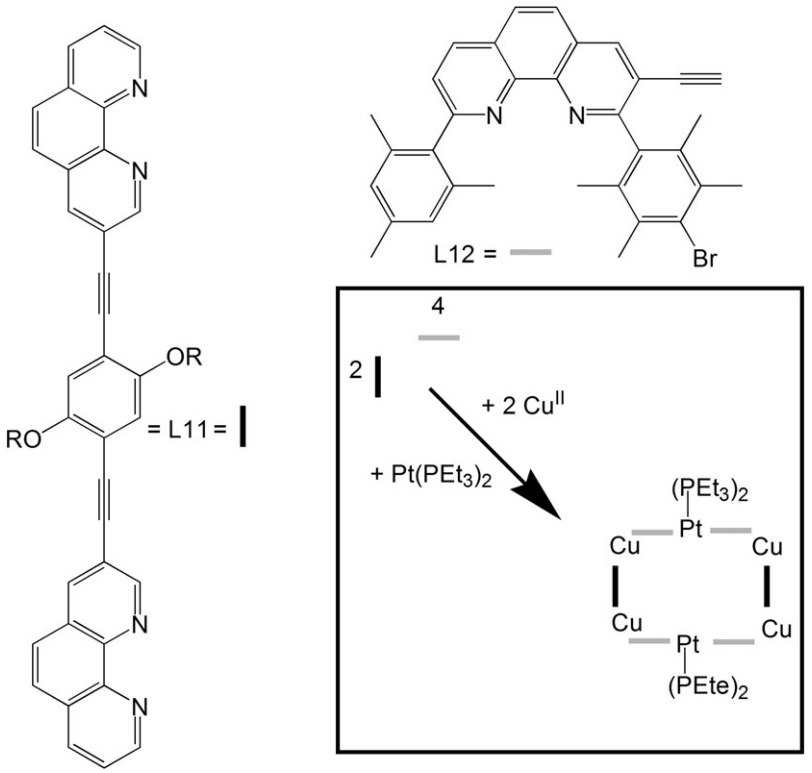

Scheme 1 Formation of the supramolecular rack $[Cu_4Pt_2]$.

indicate that the wheel exhibits frequency-dependent ac magnetic susceptibility. This means that such cyanide bridged wheels may potentially exhibit SMM behaviour.

Supramolecular nanogrids were prepared from dynamic supramolecular racks through the coupling of terminal alkynes using either a covalent (with $CuCl/O_2$) or a coordinative (with [*trans*- $PtCl_2$ $(PEt_3)_2$]) approach. Because of the rapid equilibration of the racks and oligomeric adducts formed in the coupling process, this can selectively yield the nanogrids through an entropically driven self-repair mechanism, see Scheme 1. In fact this has proven that these building blocks (L^{11}–L^{12}) are versatile precursors to the formation of supramolecular nanostructures.[7] In this context, the ability to build large nanostructures such as squares is important and systems including chromophores are also being constructed as possible light harvesting devices.[8]

The constitutional self-selection of [2 × 2] homonuclear grids from a dynamic mixture of copper(I) and silver(I) metal complexes has been achieved. This controlled self-selection and quantitative parallel amplification of the homonuclear grid architectures is derived from the same ligand, L^{13}, of different conformational geometries and Cu^I and Ag^I metal ions of different coordination behaviour and ionic size. L^{13} carries two 2-iminopyridine functionalities and was chosen as the synthetic precursor for the double-level library. This strategy using 2-iminopyridine groups gives easy access to bifunctional bipyridine-type ligands, which generate grid-type compounds in the presence of tetrahedral metal and metal-ion binding imposes a *cisoid* arrangement of pyridine nitrogens, as is common in numerous complexes of

bipyridine. Metal-ion coordination and conformational interconversion between the *cis* and *trans* arrangements around the central phenyl moiety of the chelating sites of L^{13} act simultaneously, leading to the exchanging species in solution, see Fig. 4.[9] The control of complex formation by a combination of steric and electronic factors to form dinuclear side-by-side *vs*. tetranuclear [2 × 2] grid-type silver(I) complexes has also been demonstrated using (L^{14}).[10] Squares based upon porphyrazine-type ligands, L^{15}, have also been prepared of the form $[Pt_4(L^{15})_4]^{8+}$ which represent a novel alternative to producing nanostructures on surfaces compared to porphyrin systems.[11] Metal centres organised by the formation of a [2 × 2] grid, $[Co^{II}{}_4(L^{16})_4]^{8+}$ [L^{16} = 4,6-bis(2,2′-bipyrid-6-yl)-2-phenylpyrimidine] have been addressed using STM/STS. The complex was deposited onto highly oriented pyrolytic graphite (HOPG), with the aim of achieving STM studies on an isolated [2 × 2] grid. At very low coverage, the molecules align preferably with the step edges of the HOPG surface and STS at room temperature allowed the metal centres to be addressed directly.[12] The use of STM single molecule visualization of supramolecular complexes is extremely powerful and images of the coordination-assembled porphyrin macrocycles deposited on a metal surface have also succeeded in visualizing the extremely large porphyrin macroring consisting of 30 porphyrins with a hollow structure[13] and highly conjugate macrocyles.[14]

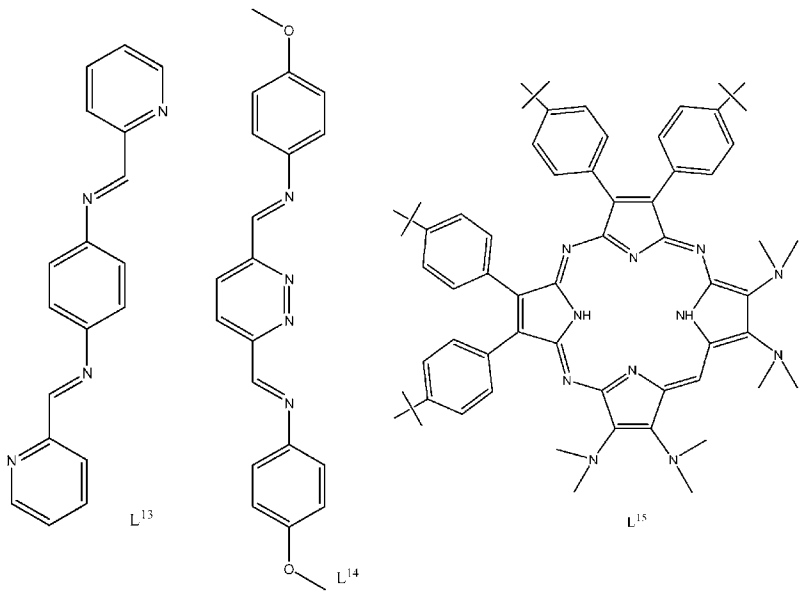

It has been shown that heterometallic wheels can be templated about tertiary amines and imidazoles, leading to new octa-, nona- and deca-nuclear rings. In extension to this work it was found that other templates lead to other rings, differing in size and metal composition. The new templates also influence the bridging ligands involved in the rings, which present the possibility of doing ligand substitution chemistry on the ring backbone in the future.[15] This implies that it should be possible to link the rings and this approach was indeed exploited for this purpose. By using a mixed $\{Cr_7Ni_1\}$ wheel and using the templating amine to bring two wheels together, it may be possible to work towards complexes that may be interesting as archetypal QBITS. In initial experiments it was shown that basic diamines of a variety of

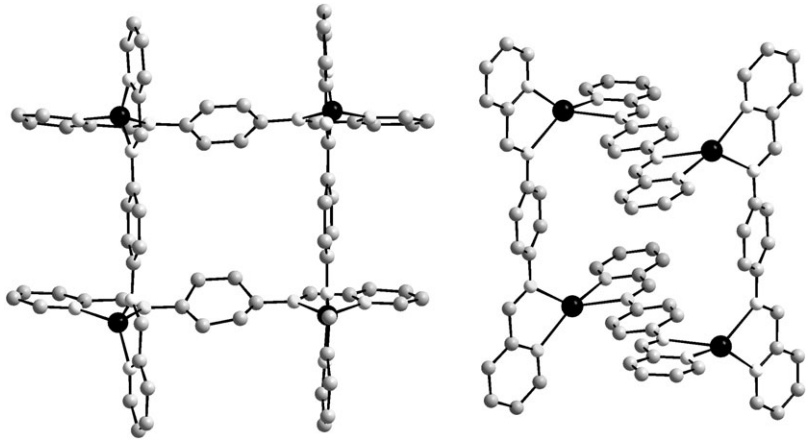

Fig. 4 Representation of the structures of the $[M_4(L^{13})_4]$ complexes: M = Cu; LHS, M = Ag, RHS.

lengths (1,8-diaminooctane, 1,9-diaminononane and 1,3-di(piperidine)propane) are able to link the clusters. However, to produce a candidate QBIT it is essential that the link between the clusters is switchable so the linked cluster $\{Cr_7Ni\text{-}NiCr_7\}$ = $[\{M_2(O_2CCMe_3)_4\}\{[EtNH_2CH_2py][Cr_7NiF_8(O_2CCMe_3)_{16}]\}_2]$ (where M = Cu, Ni, or Co) was made, see Fig. 5.[16] The idea of tuning communication between magnetic clusters can also be applied to mixed valence complexes. In this case, a mixed valence complex incorporating four ferrocene units around a core has been postulated as a possible model for developing quantum cellular automata.[17]

It is possible to replace the pivaleic acid ligand (O_2CCMe_3) in the $\{Cr_7Ni_1\}$ with a range of other carboxylates. For instance, (O_2CCMe_3) can be replaced with 3-thiophenecarboxylate (L^{17}) to give clusters of the form $[NR_2H_2][Cr_7NiF_8(L^{17})_{16}]$.[18]

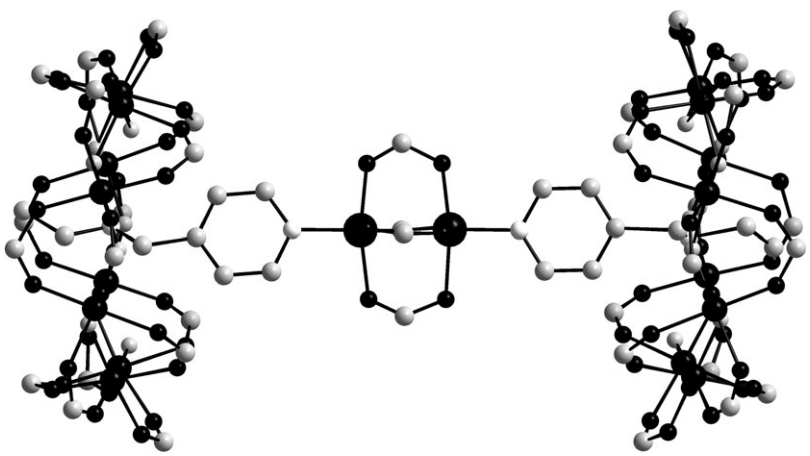

Fig. 5 Representation of the structure of $[M_2(O_2CCMe_3)_4]\{[EtNH_2CH_2py][Cr_7NiF_8(O_2CCMe_3)_{16}]\}_2]$. The $CCMe_3$ groups are removed from this structure.[16]

A molecular pinwheel multicopper(I) cluster, $[(L^{18})_6Cu^{I}_{13}(S^{2-})_2]^{3+}$ with μ_4-sulfido, μ_3-thiolato ligands has been synthesised from HL^{18} and copper(I) and the cluster contains the first example of a distorted pyramidal Cu_4S core.[19]

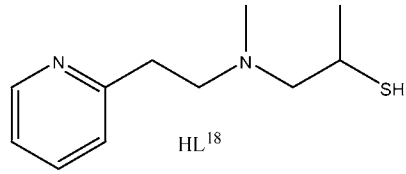

HL^{18}

The reaction of $[Mn_{12}O_{12}(O_2CCH_3)_{16}(H_2O)_4]$ with H_2L^{19}, H_2L^{20} or H_2L^{21} leads to the formation of wheel-shaped $[Mn^{III}_6Mn^{II}_6]$ complexes with the general formula $[Mn_{12}(L)(O_2CCH_3)_{14}]$ (L can be = L^{19-21}). The spin ground states of the three resulting complexes were found to be S = 8, g = 2.0, and D = -0.47 cm^{-1} for L^{19}; S = 8, g = 2.0, and D = -0.49 cm^{-1} for L^{20}; and S = 8, g = 2, and D = -0.37 cm^{-1} for L^{21}. The ac magnetic susceptibility data were measured for the complexes and slow kinetics of magnetization reversal relative to the frequency of the oscillating ac field were observed as frequency-dependent out-of-phase peaks.[20] The complexation of *N*-methyldiethanolamine (H_2L^{19}) with Fe^{III} and Ni^{II} salts yields $\{Fe_{22}\}$ and $\{Ni_{24}\}$ clusters, respectively. The iron cluster was formulated as: $[Fe_{22}O_{14}(OH)_3(O_2CMe)_{21}(L^{19})_6]^{2-}$ and forms in a 20% overall yield. The structure is unprecedented and consists of 22 Fe(III) ions arranged in three sub-units; this is the largest homometallic Fe cluster to date. There is a central $[Fe_4(\mu_3\text{-}OH)_2(\mu_4\text{-}O)_2]^{6+}$ cubane, which is a very rare unit at this oxidation level, see Fig. 6.[21] The same ligand forms a $\{Ni_{24}\}$ cluster $[Ni_{24}(O_2CMe)_{42}(L^{19})_6(EtOH)_6]$ and the complex consists of a $\{Ni_{18}\}$ loop to which are connected six additional Ni(II) atoms. All the Ni atoms have distorted octahedral geometry, and the loop has a chair-like conformation.

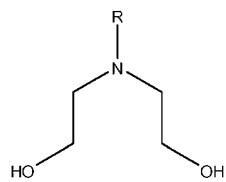

R = -CH_3 H_2L^{19}
-CH_2CH_3 = H_2L^{20}
-$CH_2CH_2CH_2CH_3$ = H_2L^{21}

The first cobalt metallacrowns and inverse metallacrowns have been reported *via* the reaction of cobalt(II) acetate with di-2-pyridyl ketone oxime (HL^{22}) in the presence of ClO_4^- and PF_6^- counterions.[22] Hexanuclear, octanuclear, and decanuclear manganese metalladiazamacrocycles have also been reported.[23]

Mulitnuclear Au complexes have been of interest.[24,25] For instance, a chiral luminescent $\{Au_{16}\}$ ring self-assembled from achiral components has been reported. This ring is supported by Au···Au interactions which average *ca.* 3.12 Å and is formed by the reaction of $[Au_2(L^{22})Cl_2]$ with K_2L^{23} in dry methanol at room temperature (L^{22} = bis(diphenylphosphino)methane) and L^{23} = piperazine-1,4-dicarbodithiolate), see Fig. 7.[25] This is interesting since the ring has a well defined structure, is chiral, and is supported by Au···Au interactions.

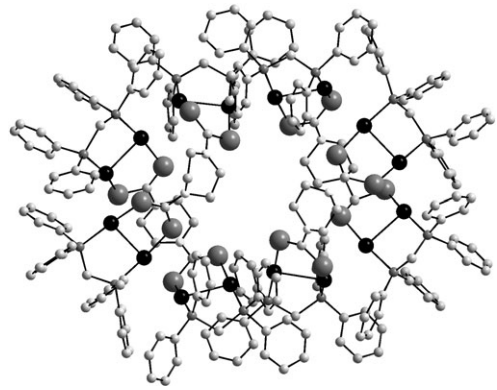

Fig. 6 Structure of the $\{Fe_{22}\}$ carbon atoms omitted for clarity. Fe —black, O—grey, N—white.

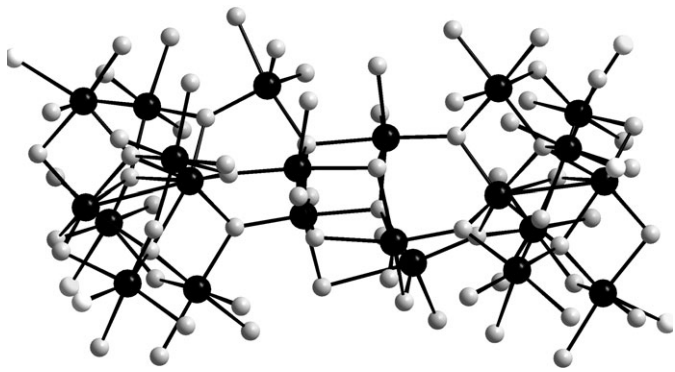

Fig. 7 The structure of the $\{Au_{16}\}$ wheel. The S atoms are show as large grey spheres, the P atoms as small grey spheres and the Au atoms as black spheres.

The first structures of simple acetate complexes of vanadium(III) formed in aqueous solution have been recently reported: $[V_4(\mu\text{-}OOCCH_3)_4(\mu\text{-}OH)_4(OH_2)_8]^{4+}$ and $[V_3(\mu_3\text{-}O)(\mu\text{-}OOCCH_3)_6(OH_2)_3]^{1+}$. These clusters were confirmed to exist in both solution and the solid state. The $\{V_4\}$ core consists of four equivalent distorted octahedral V^{III} centres, each centre coordinated to two μ-hydroxo ligands, two μ-acetato ligands, and two aqua ligands. The four vanadium(III) centres lie within a plane, with the μ-acetato and μ-hydroxo ligands lying above and below the plane, respectively, in an alternate arrangement around the ring. The $\{V_3\}$ has the same structure as the classical oxo-centred trimers with 6 bridging acetate ligands and three water molecules, see Fig. 8.[26]

A novel $\{Cu_3H\}$ complex capped by three diphosphine ligands has been discovered that is stable and has interesting photoluminescent properties. The complex is formed by the reaction of the copper complex of bis(dicyclohexylphosphino)-methane (L^{24}), $[Cu_2(L^{24})_2]^{2+}$, with MeOH in the presence of KOH. This affords the hydride complex $[Cu_3(L^{24})_3(\mu_3\text{-}H)]^{2+}$, see Fig. 9.[27]

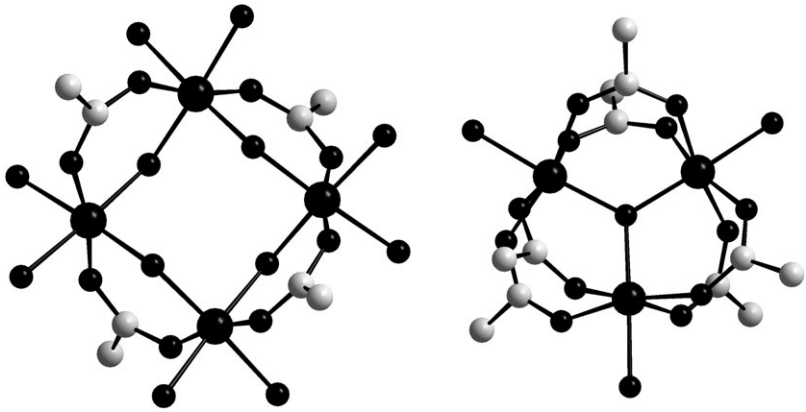

Fig. 8 Structures of the $\{V_4\}$ (LHS) and $\{V_3\}$ (RHS) clusters.

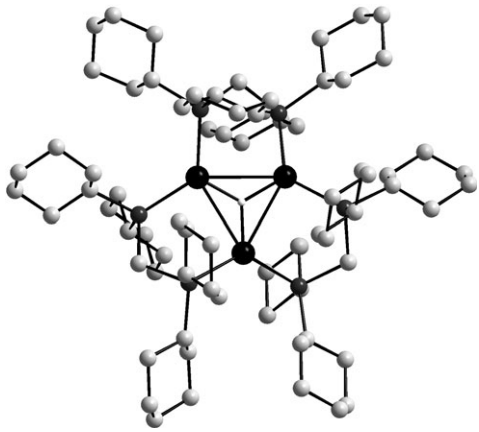

Fig. 9 A representation of the structure of $[Cu_3(L^{24})_3(\mu_3\text{-}H)]^{2+}$.

3. Cluster frameworks and cages

An azine-bridge octanuclear copper(II) complex is assembled from the one-stranded ditopic thiocarbohydrazone, H_2L^{25}, to give $[Cu_8(L^{25})_4(DMF)_8(H_2O)]$. The unprecedented octanuclear cluster is formed by a unique heptadentate ligand that exhibits a particular conformational and configurational flexibility, appropriate spatial arrangement of metal-binding sites, coordination ability, and acid–base properties which allow full use of its donor capacity to fulfil the coordination requirements of the metal ions with minimum strain.[28] The use of conformationally flexible ligands to form helicates has been used to great effect in supramolecular chemistry. Recently, the molecular recognition of a three-way DNA junction was discovered to occur *via* an unprecedented supramolecular helicate-DNA major groove interaction. The helicate has the composition $[Fe_2(L^{26})_2]^{4+}$ and binds palindromic hexanucleotide, 5′-d-(CGTACG)-3, at a three-way junction which forms a triangular-shaped hydrophobic binding site, see Fig. 10. The structure reveals that the nanoscale supramolecular triple-helical antiprism is similarly matched to the size and shape of the cavity in the three-way DNA junction. Further, it demonstrates that such a three-way

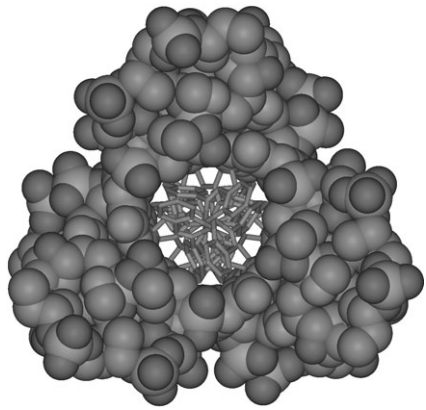

Fig. 10 A representation of the structure of the three-way DNA junction (shown in space filling) encapsulating the helical $[Fe_2(L^{26})_2]^{4+}$ (shown in sticks) LHS.

DNA junction structure is an appropriate target for the design of a new family of ligands with a high structural specificity and strong-binding characteristics.[29]

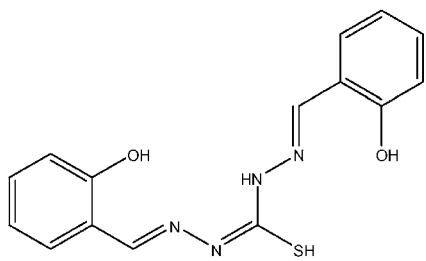

H4L25

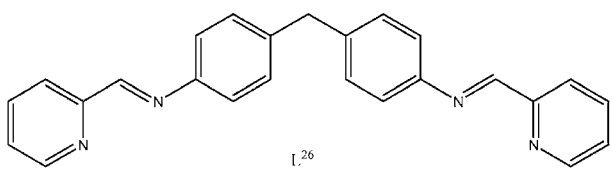

L^{26}

The isolation and characterization of the first circular single-stranded polymetallic lanthanide-containing helicate has been accomplished. The complex forms a triangular species, see Fig. 11, $[Eu_3(L^{27})_3]^{5+}$, and the purity of the complex is confirmed by a range of analytical techniques.[30] In a similar context an interesting structural diversity in the assembly of helicate-type nickel(II) complexes with enantiopure *bis*(β-diketonate) ligands has also been reported.[31] Further, a dinuclear triple-stranded helicate with a bis(benzene-o-dithiolato)-type ligand has been constructed by the reaction with Ti^{IV} in a self-assembly reaction to give the dinuclear triple-stranded

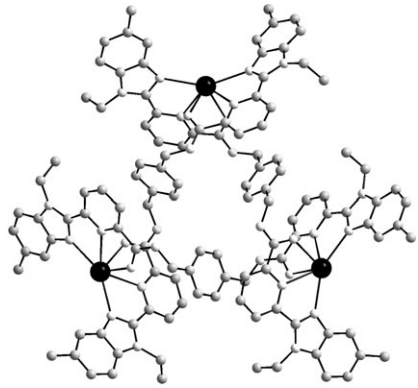

Fig. 11 Structure of $[Eu_3(L^{27})_3]^{5+}$ helicate.

helicate and this work is the first helicate to be built exclusively from benzene-o-dithiolato donor groups.[32]

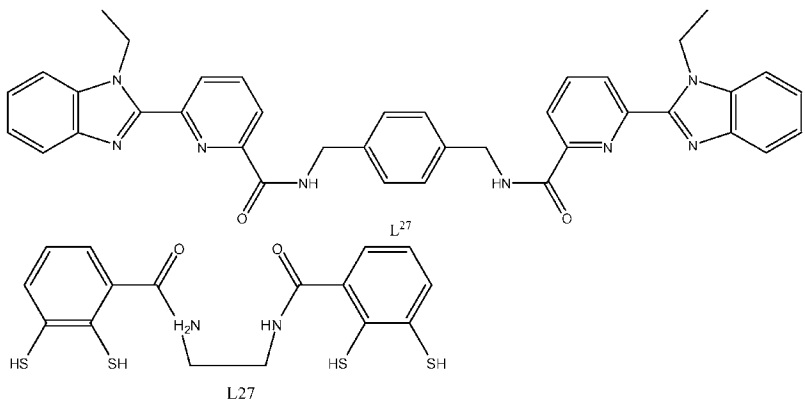

The development of stable helical lanthanide complexes continues to be an important aim and a trinuclear Eu^{III} array within a diastereoselectively self-assembled helix has been formed using a chiral bipyridine-carboxylate ligand (HL^{28}). This ligand features a carboxylate donor group appended to the pinene moiety to take advantage of the oxophilic character of Ln^{III} ions. Besides increasing the stability of the lanthanide complexes, the carboxylate group may also serve to enhance the transmission of the chiral information to the final supramolecular architecture. In this context it was discovered that a trinuclear array can be self assembled with this ligand and Eu^{III} ions with complete diastereoselectivity to yield the complex as: $[Eu_3(+\text{-}L^{28})_6(\mu_3\text{-}OH)(H_2O)_3]$. This complex displays a very

interesting mode of helical chirality that originates from the propeller-like arrangement of the ligands around the trinuclear metal core, see Fig. 12.

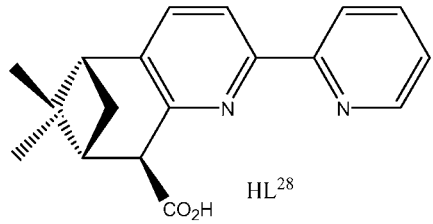

HL^{28}

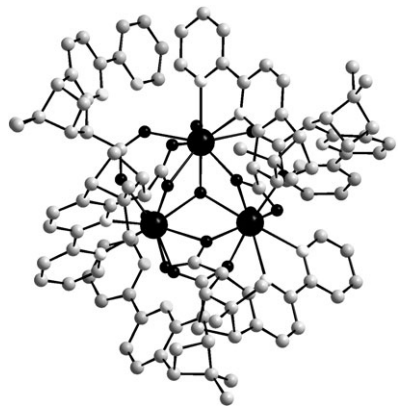

Fig. 12 A representation of the structure of $[Eu_3(+\text{-}L^{28})_6(\mu_3\text{-}OH)\text{-}(H_2O)_3]$.

Rare earth complexes of nitrogen based ligands (L^{29}) have also been used to form a dimeric lanthanum hydroxo-based complex that can fix atmospheric CO_2 to form an unusual hexameric carbonate. *i.e.* exposure of $[La(L^{29})(\mu\text{-}OH)]_2(\mu\text{-}\eta^1\text{:}\eta^1\text{-}OTf)]^{3+}$ to air results in the immediate uptake of atmospheric[33] CO_2 and the reaction of lanthanide trichloride hexahydrates $[LnCl_3 \cdot 6H_2O]$ (Ln = Yb, Lu) with two equivalents of benzoylferrocenoylmethane (L^{30}) resulted in a tetranuclear lanthanide hydroxo cluster which is made up of a distorted tetranuclear lanthanide Ln_4O_4 cubane core. Notably, this compound contains the maximum number of ferrocene units anchored to any molecular metal–heteroatom framework structurally reported.[34]

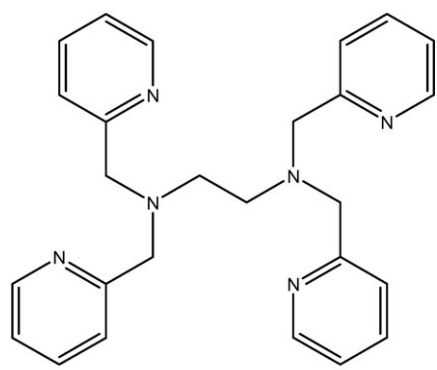

L^{29}

The development of nanoscale cages has continued to advance. For instance, the rational design of a coordination cage with a trigonal-bipyramidal geoemtry has been constructed from 33 building blocks. The structure is based upon the ligands *tris*(2-hydroxybenzyl)triaminoguanidinium (L^{31})[35] and 5,5-diethylbarbiturate (L^{32}), and their complexation with $PdCl_2$ to yield $[Pd_3(Br_3L^{31})_6(\mu\text{-}L^{32})_9]^{12-}$. The ligand, L^{31}, is C_3-symmetric and covers six faces of the trigonal bipyramid. To construct even larger cages with more building units, this design principle was followed, but in addition to metal centres for the linkage along the edges, a second twofold bridging ligand, L^{32} was also used, see Fig. 13.[36]

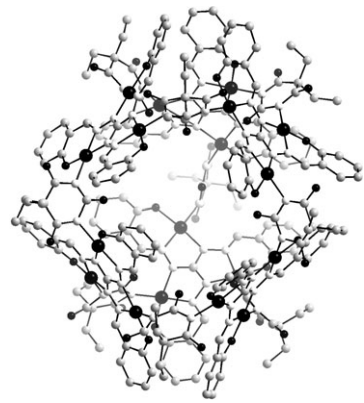

Fig. 13 Structure of $[Pd_3(Br_3L^{31})_6(\mu\text{-}L^{32})_9]^{12-}$.

Host–guest interactions also allow a design strategy to be developed using templating effects. For instance cobalt(II) complexes of L^{33} synthesised in the presence of BF_4^- allows the templation of some unusal coordination cages.[37] The use of a chiral bridging ligand affords a single diastereoisomer of a tetrahedral $M_4(L^{34})_6$ cage complex in which the optical rotation of each ligand is increased by a factor of 5 on coordination.[38] The diastereoselective formation of a coordination cage, $[Zn_4(L^{34})_6](BF_4)_8]$, has been achieved using a chiral bridging ligand and results in substantial chiral amplification associated with adoption by all of the ligands of a helical conformation upon binding. The formation of tetrameric clusters using related ligands has also been reported.[39] Further, the reaction of ligands L^{35} and L^{36} with $Cu(BF_4)_2$ in a 3:3:1 ratio in nitromethane afforded green crystals of $[Cu_{12}(\mu\text{-}L^{35})_{12}(\mu_3\text{-}L^{36})_4]^{24+}$ which has a cuboctahedral metal framework containing eight triangular and six square faces. The complex lies on a C_2 axis. Four of the eight triangular faces are capped by a triply bridging ligand, L^{36}, and the remaining vacant edges are spanned by doubly bridging ligands, L^{35}. All 12 *tris*-chelate metal centres have meridional geometry, and all have the same chirality, indicating that the same chiral configuration at each metal centre is necessary for the closed cage to form, and the central cavity (*ca.* 450 Å^3) contains disordered anions and solvent, see Fig. 14.[40]

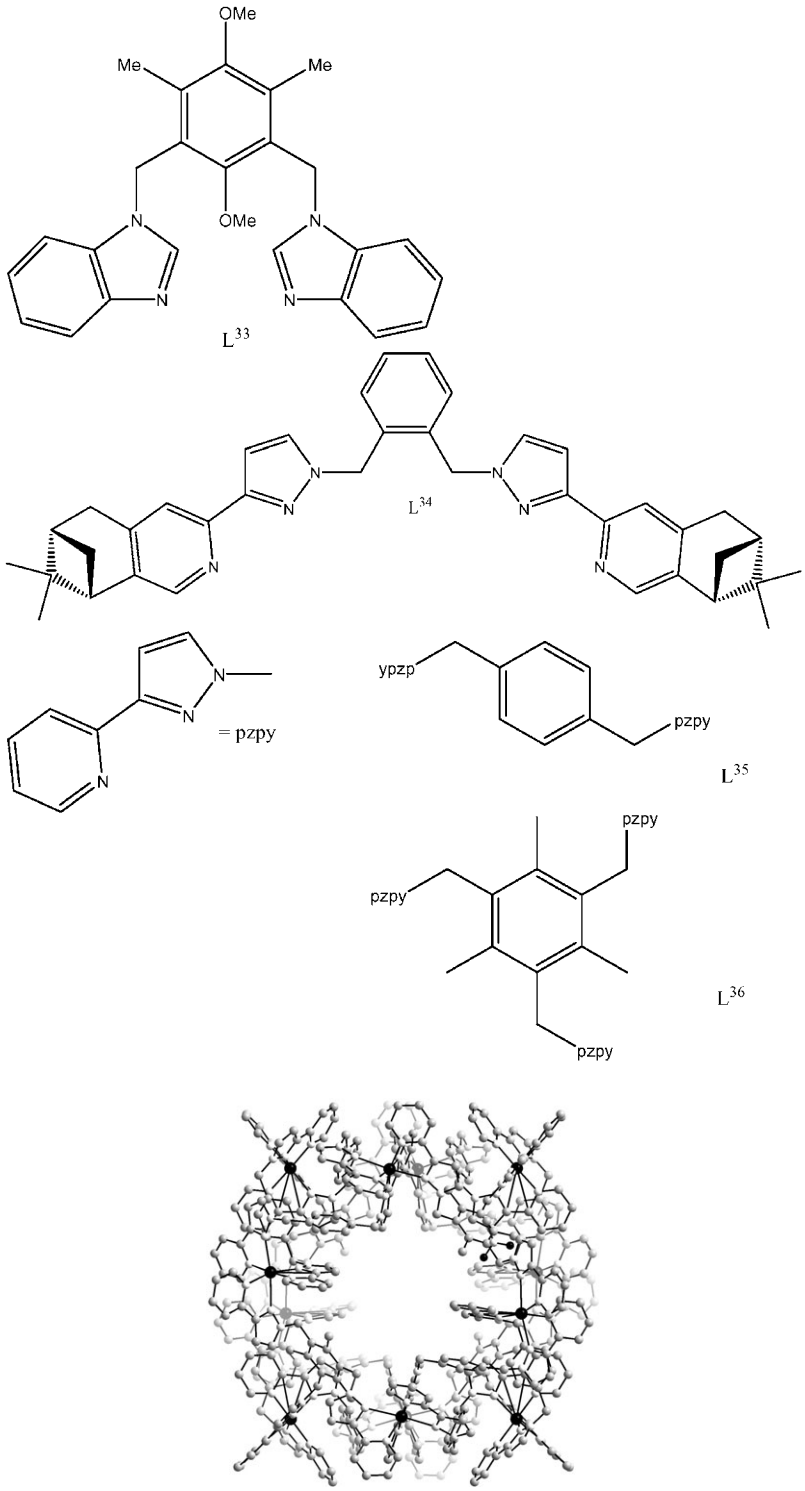

Fig. 14 Structure of $[Cu_{12}(\mu\text{-}L^{35})_{12}(\mu_3\text{-}L^{36})_4]^{24+}$ with a 450 Å^3 cavity.

A metallosupramolecular prism is formed from the coordination of cyclotriveratrylene-type ligands with silver giving a dimeric capsule: $[Ag_2(tris(3\text{-pyridylmethylamino})cyclotriguaiacylene)_2(CH_3CN)_2]^{2+}$ with *tris*(3- pyridylmethylamino)-cyclotriguaiacylene) (L^{37}) and a tetrameric capsule $[Ag_4(tris(4\text{-pyridylmethylamino})cyclotriguaiacylene)_4(CH_3CN)_4]^{4+}$ with (*tris*(4-pyridylmethylamino)cyclotriguaiacylene) (L^{38}). The latter features a tetrahedral metallosupramolecular prism whereby the utilization of the more divergent 4-pyridyl ligand leads to the formation of a significantly expanded stellated tetrahedron with an internal space capable of accommodating 5 CH_3CN guest molecules.[41] The synthesis of a cavitand based coordination capsule that can encapsulate aromatic guests as well as aliphatic guests has been synthesised. The chiral variation of the capsule can encapsulate a chiral guest to show diastereoselection.[42] Deep cavitands have also been selectively constructed by controlling the order of addition of the cavitand ligands[43] and anion template effects on the self-assembly and interconversion of metallacyclophanes have recently been discovered.[44]

Zn-II-salphen complexes are readily accessible and interesting supramolecular building blocks with a large structural diversity have been reported. Interestingly, it has been found that the box assemblies line up in the solid state to form porous channels that are potentially useful in a number of applications.[45] A [3 + 3] modular self-assembly gives rise to the formation of basket-shaped, crown ether-functionalized, nano-sized trimetallo-macrocycles.[46]

Nanoscale capsules provide a well defined reaction space for reaction chemistry, through the encapsulation of smaller guest molecules. This is because it is possible to both tune the environment of the inner space and because it may be very different from that of the exterior surroundings, allowing access to new chemistry *via* the stablisation of reactive intermediates, for example. $[CpRuCl(L^{39})]$ (L^{39} = 1,5-cyclooctadiene), a catalyst employed in many C–C bond-forming reactions, was encapsulated in a $[Ga_4(L^{40})_6]^{12-}$ capsule (see Fig. 15) to give $[CpRu(L^{39})(H_2O) \subset Ga_4(L^{40})_6]^{11-}$. Interestingly, the $CpRu(L^{39})(H_2O)$ species is extremely stable inside the host (for weeks) whereas normally the species decomposes within minutes in the presence of water.[47] Further, it has been shown that guests can be incorporated into the $[Ga_4(L^{40})_6]^{12-}$ tetrahedron *via* 'pores' and a guest can extend out of the cavity.[48]

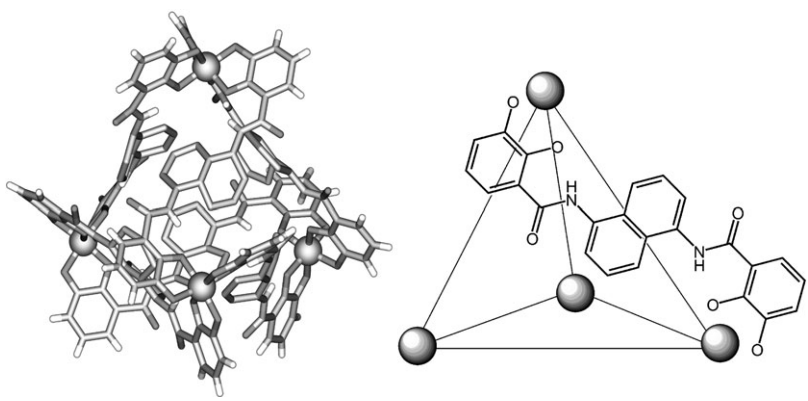

Fig. 15 Left: A schematic structure of $[Ga_4(L^{40})_6]^{12-}$. Right: A scheme showing the binding mode of the ligand, L^{40}.

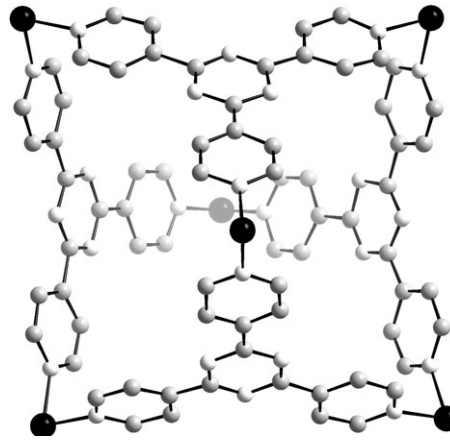

Fig. 16 Representation of structure of **1**, $\{[(Pd)en]_6(L^{43})_4\}^{12+}$ where L^{42} = 2,4,6-tris (4-pyridyl)-1,3,5-triazine and the Pd(II) ions lay at the corners of an octahedron. The en moieties and guest are omitted for the sake of clarity.

Guest exchange *via* the 'pores' has been investigated, and it is postulated that this can occur without rupture of the host cavity through ligand dissociation.[49]

As an extension to a rational design for the formation of self-assembled coordination cages, the syntheses for very large M_4L_4 tetrahedra based on a hexadentate 3-fold symmetric ligand (1,3,5-tris(4′-(2″,3″-dihydroxybenzamido)phenyl)benzene (H_6L^{41})) has been investigated and this forms a range of new complexes.[50] A_4B_6 compounds have also been synthesized enantiospecifically by employing the trianion of benzene-1,3,5-tricarboxylic (L^{42}) acid as "A" and the $[R\text{-}cis\text{-}Rh_2(C_6H_4PPh_2)_2]^{2+}$ cation as "B".[51] One of the most important coordination cages with a well defined nanospace is based on the coordination of six Pd(II) centres and four 2,4,6-tris (4-pyridyl)-1,3,5-triazine, L^{43}, and has the composition $[(PdB)_6(L^{43})_4]^{12+}$ (B = a bidentate blocking group like $[enPd(II)]^{2+}$ or 2,2′-bipyridine). This $[Pd_6(L^{43})_4]$ capsule also has a large hydrophobic cavity, yet the outer part is hydrophilic, see Fig. 16. It is also possible to synthesise similar vessels, but with endohedral functionalisation and these have been referred to as 'endomers'.[52] The tri-coordinated ligand, L^{43}, is rather electron-deficient within the capsule, therefore, the cavity binds preferentially electron-rich aromatic guests and this stereochemically well defined cavity shows great ability to control chemical reactions. For example, Diels–Alder reactions are dramatically accelerated by a factor of >100, and [2 + 2] photodimerization of olefins react with high regio- and stereo-selectivity and the rate is accelerated. This has been observed crystallographically when the olefin photodimerization reaction takes place *via* thermal molecular tumbling within the cavity. In fact, *in situ* crystallographic studies reveal that the solid state [2 + 2] photodimerization of acenaphthylene in a coordination cage takes place smoothly without preorganization of reaction centres at a preferred geometry, because the substrate tumbles thermally in the large hollow of the cage: *i.e.* the cavity provides organic substrates with a solution-like environment even in the crystalline state. Due to the rigid framework of the cage, the crystallinity remains unchanged even after 100% conversion of the reactant in the cage, allowing the *in situ* crystallographic observation of the photochemical transformation.[53] The formation of "molecular

ice'' within variants of $[Pd_6(L^{43})_4]$, whereby ten water molecules are complexed within the cavity[54] may help further the understanding of the reactivity and host–guest binding properties of such capsules. Indeed, the sequence specific binding of tri-peptides has been observed within the $[Pd_6(L^{43})_4]$,[55] whereby Trp-Trp-Ala was favoured over other sequences and singly mutated tri-peptides. By changing the ligand from L^{43} = 2,4,6-tris(4-pyridyl)-1,3,5-triazine to 2,4,6-tris(3-pyridyl)-1,3,5-triazine (L^{44}), it is possible to make an open bowl, $[Pd_6(L^{44})_4]$-type complex, which can form a dimeric capsule by binding both ends of a nine-residue peptide (Trp-Ala-Glu-Ala-AlaAla-Glu-Ala-Trp; 2). NMR titration experiments revealed that the monomeric bowl recognized two Trp residues.[55] Furthermore this cage has been used to directly observe a coordinatively unsaturated manganese complex, $Mn(L^{45})(CO)_3$ (L^{45} = methylcyclopentadienyl), that liberates CO *via* photodissociation in the crystalline state, and *in situ* generated $Mn(L^{45})(CO)_2$ is directly observed by X-ray diffraction. The crystallographic analysis clearly concludes that the 16-electron unsaturated manganese complex adopts a pyramidal geometry.[56]

The design of a similar cage, involving two 2,4,6-tris(4-pyridyl)-1,3,5-triazine, L^{43}, and three 4,4′-bipy ligands with six $[enPd(II)]^{2+}$ as corner units yields a pillared cylinder that has interesting guest binding properties by virtue of the organic-pillared nature of the cylinder being able to complex *via* a combination of interactions. The complexation of tetrathiafulvalene (TTF) allowed the generation of a mixed-valence radical dimer cation within the self assembled cage.[57] This is significant since this non-covalently bound species can only be generated in such a cage or by covalent linking where a similar effect is also observed by using the cavity to complex large planar aromatic organic molecules,[58] as well as cause the stacking of $M(II)(acac)_2$ (M = Pt, Pd, Cu) moieties which exhibit M–M interactions.[59]

A porous metal-organic truncated octahedron has been constructed from paddle-wheel squares and terthiophene links. These paddle-wheel units were prepared by the reaction of $Cu_2(CO_2)_4$ building blocks in which the carboxylate carbon atoms defined a rigid square and 2,2′:5′2″-terthiophene-5,5″-dicarboxylate (L^{46}) having a linking angle very close to 90° when in the *cis,cis* confirmation. The resulting cluster is formed as: $[Cu_{12}(L^{46})_{12}(L^{47})_6(H_2O)_6]$ where L^{47} = 2-methyl-1-pyrrolidinone. The material formed by the crystallisation of this capsule is extremely porous where solvent accessible area accounts for *ca.* 68% of the crystal volume, see Fig. 17.[60]

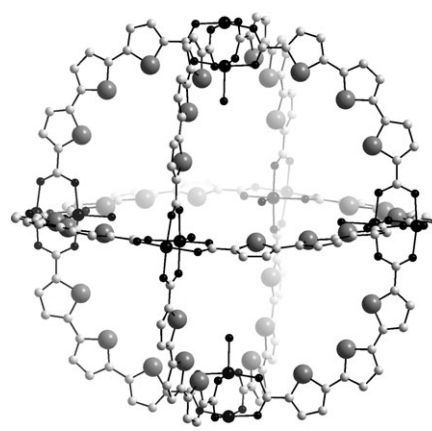

Fig. 17 Representation of the structure of $[Cu_{12}(L^{46})_{12}(L^{47})_6(H_2O)_6]$.

Face-driven corner-linked octahedral nanocages formed by C_3 symmetric triangular facial ligands linked *via* C_4-symmetric square tetratopic Pd^{II} ions at truncated octahedron corners have been reported. The use of suitably designed C_3-symmetric facial ligands and C_4-symmetric metal ions as a general strategy for the preparation of face-driven corner-linked truncated octahedral nanocages has been adopted. The cage, $[Pd_6(L^{48})_8]^{12+}$ (L^{48} = *N*,*N*′,*N*″-*tris*(3-pyridinyl)-1,3,5-benzenetricarboxamide), was prepared with eight C_3-symmetric tridentate ligands. The combination of the nitrogen donor atom at the meta position of the carboxamido pyridinyl group and the tilted pyridyl versus the facial plane of the ligand can provide the needed curvature for the formation of an octahedral cage. The nitrogen atoms can coordinate to the square planar palladium(II) ions to form kinks with approximately 120° angles at the C_4-symmetric square planar corners of the truncated octahedron, see Fig. 18.[61]

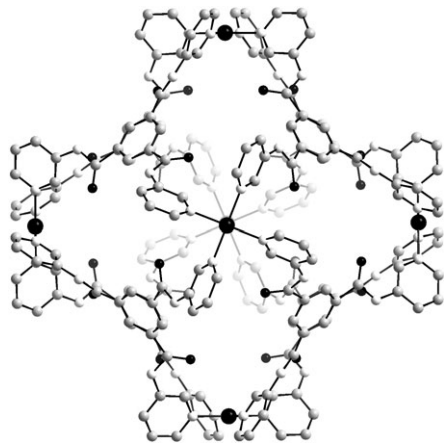

Fig. 18 Structural representation of $[Pd_6(L^{48}{}_8]^{12+}$.

By using a complex as ligand approach, the metal-ion-templated self-assembly of heterometallic tetranuclear metallomacrocycles containing kinetically locked Ru^{II} centres with a 2,2′:4,4″:4′,4‴-quaterpyridyl ligand (L^{49}) has been achieved. Depending on the metal-ion template employed in the self-assembly process, the final macrocycle can be kinetically labile or inert. Host–guest studies carried out with the same macrocycle in organic solvents reveals that the complex functions as a luminescent sensor for anions and that binding affinity and luminescent modulation is dependent on the structural nature and charge of the guest anion.[62]

Designing and discovering coordination clusters based on manganese is still a highly studied area. The basic principle here is that paramagnetic metal ions linked together in triangular arrays may lead to molecules with large spin ground states. $[Mn_4O_6]^{4+}$ aggregates also provide a route to new clusters[63] as do phosphonate-based manganese cage structures[64] and routes involving reductive aggregation reactions are reported.[65] If the cluster arrays consist of simple $\{M_3\}$ equilateral triangles then the resultant competing exchange interactions or spin frustration may stabilize a nonzero spin ground state. If the arrays consist of $\{M_4\}$ centred triangles or "metal stars", in which the three peripheral ions are connected only to the central ion and not to each other, then the antiferromagnetic interaction between these ions may stabilize a large spin state. Further, if these high-spin triangular units can then

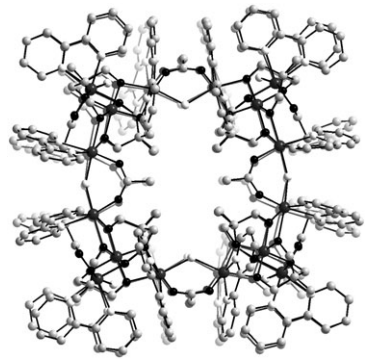

Fig. 19 Structural representation of $[Mn_{32}(L^{19})_{16}(bpy)_{24}(N_3)_{12}(OAc)_{12}]^{8+}$.

be linked together by using bridging ligands that promote ferromagnetic exchange then the resultant complexes could well be characterized by extremely large spin ground states. To help encourage these interactions, a ligand design approach using the tripodal alcohol ligand, 1,1,1-tris(hydroxylmethyl)ethane (L^{19}), was developed. The resulting cation, $[Mn_{32}(L^{19})_{16}(bpy)_{24}(N_3)_{12}(OAc)_{12}]^{8+}$ consists of eight $\{M_4\}$ centered triangles linked together to form a truncated cube. Each $[Mn_4(L^{19})_2]^{4+}$ corner unit consists of a central Mn^{4+} ion and three peripheral Mn^{2+} ions. The Mn^{2+} ions are linked to the Mn^{4+} ion through the μ_2-oxygen arms of two L^{19} ligands, which sit directly above and below the $[Mn^{IV}Mn^{II}_3]$ plane, see Fig. 19. Preliminary magnetic studies revealed that the complex has a spin ground state of S = 9 (or 10).[66] The reaction of $[Mn_3O(O_2CMe)_6(py)_3]$ with the tripodal ligand HL^{49} affords the enneanuclear complex $[Mn_9O_7(O_2CCH_3)_{11}(L^{49})(py)_3(H_2O)_2]$. The metallic skeleton of the complex comprises a series of 10 edge-sharing triangles that describes part of an idealized icosahedron. Variable temperature direct current (dc) magnetic susceptibility data collected in the 1.8–300 K temperature range and in fields up to 5.5 T were fitted to give a spin ground state of S = 17/2 with an axial zero-field splitting parameter D = −0.29 cm^{-1}. Ac susceptibility studies indicate frequency-dependent out-of-phase signals below 4 K and an effective barrier for the relaxation of the magnetization of U-eff = 27 K. Magnetic measurements of single crystals of the complex at low temperature show time- and temperature-dependent hysteresis loops which contain steps at regular intervals of field; in addition inelastic neutron scattering (INS) studies confirm the S = 17/2 ground state and analysis of the INS transitions within the zero-field split ground state leads to determination of the axial anisotropy, D = −0.249 cm^{-1}, and the crystal field parameter, B-4(0) = 7(4) × 10^{-6} cm^{-1}.[67]

The reaction of $Mn(ClO_4)_2$ with 3(5)-methyl-5(3)-(2-hydroxyphenyl) pyrazole (L^{50}) yields a highly asymmetric octanuclear manganese(III) cluster, $[Mn_8(\mu_4\text{-}O)_4(L^{50})_8(thf)_4]$, resulting from the different bridging coordination modes of L^{50}.[68] Whereas the use of di-2-pyridyl methanediol, L^{51}, allows the formation of a manganese cluster with a metallacryptand shell that encapsulates a manganese oxide core; *e.g.* $[Mn^{II}_4Mn^{III}_{22}(L^{51})_{12}(OCH_3)_{12}O_{16}(OH)_2(H_2O)(OCH_3)_3]^+$, see Fig. 20. Variable temperature direct current magnetic susceptibility measurements on the cluster indicate a paramagnetic ground state that results from an overall antiferromagnetic interaction in the cluster, and variable-temperature alternating current magnetic susceptibility measurements imply it behaves as a single-molecule magnet.[69]

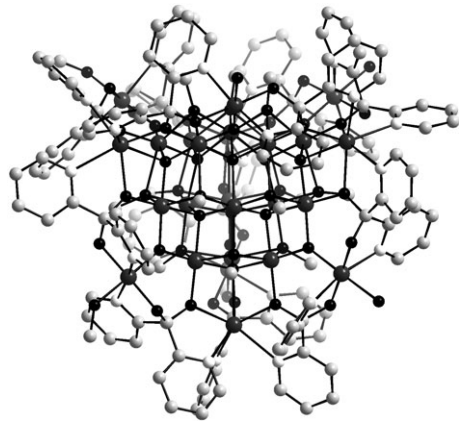

Fig. 20 A representation of the structure of $[Mn^{II}_4Mn^{III}_{22}(L^{51})_{12}(OCH_3)_{12}O_{16}(OH)_2(H_2O)(OCH_3)_3]^{+}$.

A heterometallic single-molecule magnet of $[Mn^{III}_2Ni^{II}_2Cl_2(L^{52})_2]$ where L^{52} = *N*-(2-hydroxybenzyl)-3-amino-1-propanol has been prepared. The structure consists of an incomplete face-sharing double cube that is composed of two Mn^{III} and two Ni^{II} ions.[70] An S = 6 cyanide-bridged octanuclear $\{Fe^{III}_4Ni^{II}_4\}$ complex that exhibits slow relaxation of the magnetization has been discovered. Further, as part of a continuing effort to prepare magnetic and photomagnetic cyanometalate clusters, a series of functionalized tris-(pyrazolyl)borate and -methane ligands and their cubic $Fe^{III}_4Ni^{II}_4$ cyanometalate cluster derivatives have been prepared, to probe possible relationships between molecular symmetry and blocking temperatures within a given structural archetype.[71] Slow relaxation of magnetisation in an octanuclear cobalt(II) phosphonate cage complex was found and the compound is made from hydrated cobalt nitrate reacted with two equivalents of 6-chloro-2-hydroxypyridine (L^{53}), one-sixth of an equivalent of $PhPO_3H_2$ (L^{54}) and two and one-third equivalents of triethylamine in MeCN. The resulting complex is $[Co_8(L^{53})_{10}(O_3PPh)_2(NO_3)_3(HL^{54})_2]$.[72] A Cu_2Gd heterotrinuclear complex, $[L^{54}Cu_2Gd(OAc)_3]$ (H_4L^{54} = 1,2-bis-((salicylideneamino)oxy)ethane) and the corresponding dinuclear CuGd complexes was synthesised. The trinuclear complex has a S = 9/2 ground state which results from the ferromagnetic interaction among the Cu-II-Gd-III-Cu-II triad.[73] A two-step spin conversion in a cyanide-bridged ferrous square was found that composed of a tetranuclear macrocycle built from four cyanide-bridged Fe^{II} ions, and the overall geometry is almost square.[74] Transition-metal complexes with a cubane structure, in which the four metal ions are located in the apices of a tetrahedron, are an extensively examined class of compounds with intriguing magnetostructural properties. For that reason, the synthesis of chiral, enantiomerically pure single molecule magnets is of special interest (*e.g.* for magnetodichroism), and complexes like cubanes represent potential candidates.[75] The first icosanuclear Co^{II} cluster has been isolated and it is also a rare example of a 3d metal cluster with O and N ligation.[76] A $\{Ni_8\}$ single molecule magnet has been constructed including pyrazolinone ligands, and has also been extended to include fluoride and azide bridges.[77]

4. Polyoxometalates

Interest in the design and synthesis of chiral polyoxometalates has been recently gathering momentum driven by applications to materials and catalysis. The amplification and transfer of chirality from organic tartrate to a large polytungstate has been achieved by reacting the achiral lacunary Wells-Dawson POM unit, α-$[P_2W_{15}O_{56}]^{12-}$, which has C_{3v} symmetry with D or L-tartrate (L^{54}).[78] Given the unfavourable electrostatic interactions between these fragments a positively charged mediator, in this case Zr^{IV}, is used because of high charge and coordinative flexibility to yield the chiral POM, $\{[\alpha\text{-}P_2W_{15}O_{55}(H_2O)]Zr_3(\mu_3\text{-}O)(H_2O)(HL^{54})[\alpha\text{-}P_2W_{16}O_{59}]\}^{15-}$ (both enantiomers are available and depend on the symmetry 'printed' on to the cluster by the tartrate ligand). This is interesting since the cluster framework is chiral and is robust, see Fig. 21.

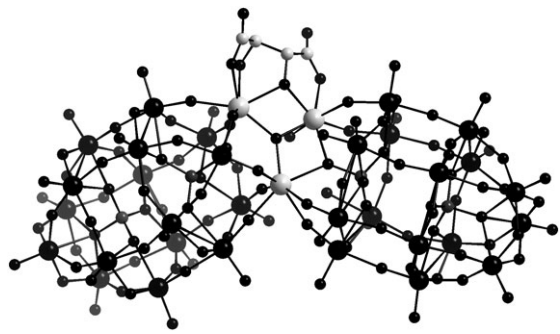

Fig. 21 Structural representation of the chiral POM $\{[\alpha\text{-}P_2W_{15}O_{55}(H_2O)]Zr_3(\mu_3\text{-}O)(H_2O)(HL^{54})[\alpha\text{-}P_2W_{16}O_{59}]\}^{15-}$ (Zr atoms in light grey).

Recently, the first examples of SO_3- based polyoxotungstates, α-$[Mo_{18}O_{54}(SO_3)_2]^{4-}$ and $[W^{VI}{}_{18}O_{56}(SO_3)_2(H_2O)_2]^{8-}$, have been discovered. The latter is described as a "Trojan Horse" in which a structural re-arrangement allows the two embedded pyramidal sulfite ($SO_3{}^{2-}$) anions to release up to four electrons (analogous to the "soldiers" hidden inside the "Trojan Horse") to the surface of the cluster generating the sulfate-based, deep blue, mixed valence cluster $[W_{18}O_{54}(SO_4)_2]^{8-}$ upon heating, see Fig. 22. The sulfite anions adopt a radically different orientation in $[W^{VI}{}_{18}O_{56}(SO_3)_2(H_2O)_2]^{8-}$ whereby they each only ligate to seven metal centres: three from the cap and four (out of six) from the "belt" of the cluster framework, see Fig. 22.[79]

The orientation for the sulfite anions within the cluster type is somewhat like the coordination mode for the tetrahedral templates ($XO_4{}^{y-}$) in conventional Dawson $[M_{18}O_{54}(XO_4)_2]^{2y-}$, *i.e.* one of the oxo ligand bridges three capping W centres, the remaining oxo ligands each bridge two of the "belt" W centres. Nevertheless, this leaves two "belt" W atoms uncoordinated to the template SO_3 moiety as SO_3 has one oxo ligand less than XO_4. Thus, it can be seen that the sulfite ions are grafted on to the bottom side of the cluster, which resembles a "basket" with four "uncoordinated" "belt" metal centres on the top part and now has a lower C_{2v} symmetry compared to the cluster α-$[Mo_{18}O_{54}(SO_3)_2]^{4-}$, which has a D_{3h} symmetry. To compensate for the coordination, these unique "uncoordinated" "belt" W centres (four for the whole cluster) each have two terminal ligands, rather than one as found

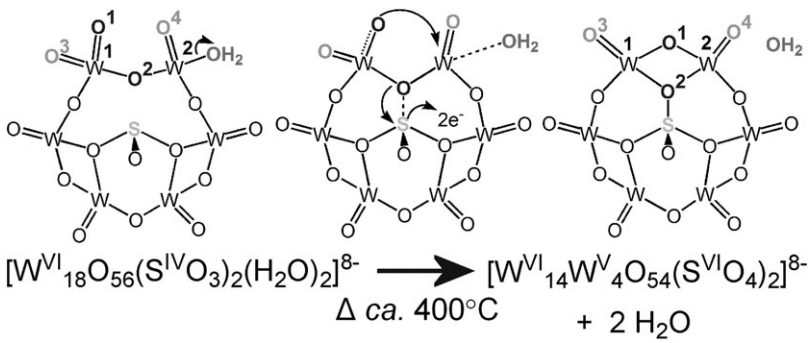

Fig. 22 Scheme showing the change in the metal oxo-framework on one half of the cluster upon oxidation of the internal SO_3^{2-} ligand to SO_4^{2-} which is commensurate with the reduction of the cluster shell by 4 electrons giving rise to the deep blue material from the colourless crystals.

for the remaining metal centres in the cluster. These are in addition to the four other μ_2 bridging oxo (O^{2-}) ligands between metal centres and complete a slightly distorted octahedral coordination geometry for each of the four ''uncoordinated'' ''belt'' metal centres concerned. Single crystal structure analysis revealed that two of the four unique metal centres each have two W═O terminals (W–O ~ 1.7 Å) and the other two each have one W═O terminal and one W–OH_2 terminal (W–O ~ 1.7 Å and ~2.2 Å, respectively). Furthermore, it is interesting that the unique ''belt'' μ_2 bridging oxo ligands between the pair of ''uncoordinated'' ''belt'' W atoms now bends in towards the cluster, rather than outwards as normal and is located *ca.* 2.9 Å distant from the sulfur centre of the SO_3 moiety, whilst the two sulfur centres are positioned 3.6 Å apart at opposite sides of the cluster shell. In this respect the mechanism for the reduction of the cluster shell proposes an interaction between the sulfur atom and the special belt oxo ligand, which then react to form two sulfate anions located within the $\{W_{18}\}$ cluster shell.[79]

In a very interesting development a late-transition metal oxo complex: $[O{=}Pt^{IV}(H_2O)L_2]^{16-}$ has been discovered where L = $[PW_9O_{34}]^{9-}$, and the authors claim to have broken the 'oxo-wall' in the isolation of the first complex to include a Pt═O moiety.[68,69] The coordination geometry around the Pt centre is described as a distorted octahedron with five Pt–O bond distances of 1.96(3) Å and one Pt═O bond distance of 1.68(3) Å, see Fig. 23.[80]

The coordination chemistry of the hexavacant tungstophosphate $[H_2P_2W_{12}O_{48}]^{12-}$ has been explored with Fe^{III} ions. In aqueous mixtures of lithium chloride and lithium acetate at ambient temperature, the reaction of $\{P_2W_{12}\}$ with an excess (8–14 equiv) of Fe^{III} chloride gives the metastable anion $[H_4P_2W_{12}Fe_9O_{56}(OAc)_7]^{6-}$. Upon heating in aqueous sodium acetate, this cluster transforms into $[H_yP_8W_{48+x}Fe_{28-x}O_{248}]^{(84-y-3x)-}$ which has been isolated as different salts that show slight variation in the value of x.[81] The first examples of polyoxometalate structures that incorporate embedded chelated heteroatoms point to new possibilities for stereochemical control of applications.[82] Clusters which display the rare cubic $\{Fe_8\}$ topology have been obtained by reaction of the metastable hexavacant polyoxotungstate $[H_2P_2W_{12}O_{48}]^{12-}$ with basic trinuclear metal acetates.[83] Two new azido-bridged polyoxometalate compounds were synthesized in acetonitrile/methanol media and their structures were determined. The

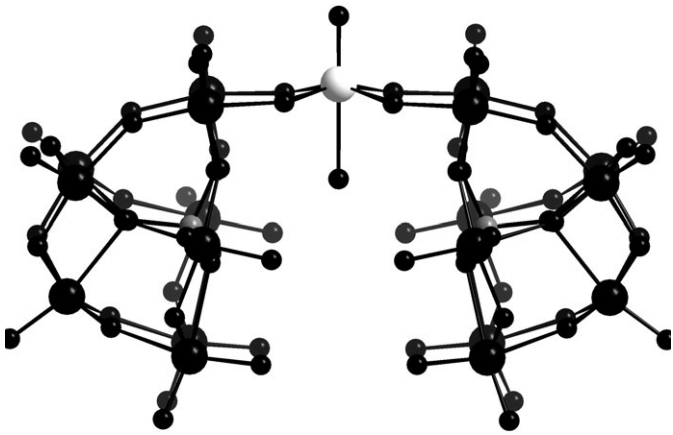

Fig. 23 The structure of the $[O = Pt^{IV}(H_2O)(PW_9O_{34})]^{16-}$ complex.

15-cobalt-substituted polyoxotungstate $[Co_6(H_2O)_{30}\{Co_9Cl_2(OH)_3(H_2O)_9(beta\text{-}SiW_8O_{31})_3\}]^{5-}$ has been structurally characterised. The trimeric polyanion has a core of nine Co^{II} ions encapsulated by three unprecedented (β-SiW_8O_{31}) fragments and two Cl^- ligands. This central assembly $[Co_9Cl_2(OH)_3(H_2O)_9(beta\text{-}SiW_8O_{31})_3]^{17-}$ is surrounded by six Co ions groups resulting in the satellite-like structure. The synthesis is accomplished in a simple one-pot procedure by interaction of Co^{II} ions with $[gamma\text{-}SiW_{10}O_{36}]^{8-}$ in aqueous, acidic NaCl medium (pH 5.4).[84] The magnetic exchange interactions in a Co-3(II) moiety encapsulated in $Na_{17}[(NaOH_2)\text{-}CO_3(H_2O)(P_2W_{15}O_{56})_2]$ were studied by a combination of magnetic measurements (magnetic susceptibility and low-temperature magnetization), with a detailed inelastic neutron scattering investigation.[85]

References

1 J. K. Tang, I. Hewitt, N. T. Madhu, G. Chastanet, W. Wernsdorfer, C. E. Anson, C. Benelli, R. Sessoli and A. K. Powell, *Angew. Chem., Int. Ed.*, 2006, **45**, 1729.
2 A. Hori, T. Sawada, K. Yamashita and M. Fujita, *Angew. Chem., Int. Ed.*, 2005, **44**, 4896.
3 N. Das, A. Ghosh, A. M. Arif and P. J. Stang, *Inorg. Chem.*, 2005, **44**, 7130.
4 H. Jude, H. Disteldorf, S. Fischer, T. Wedge, A. M. Hawkridge, A. M. Arif, M. F. Hawthorne, D. C. Muddiman and P. J. Stang, *J. Am. Chem. Soc.*, 2005, **127**, 12131.
5 M. P. Martin-Redondo, L. Scoles, B. T. Sterenberg, K. A. Udachin and A. J. Carty, *J. Am. Chem. Soc.*, 2005, **127**, 5038.
6 Z.-H. Ni, H.-Z. Kou, L.-F. Zhang, C. Ge, A.-L. Cui, R.-J. Wang, Y. Li and O. Sato, *Angew. Chem., Int. Ed.*, 2005, **44**, 7742.
7 M. Schmittel, V. Kalsani and J. W. Bats, *Inorg. Chem.*, 2005, **44**, 4115.
8 A. Sautter, B. K. Kaletas, D. G. Schmid, R. Dobrawa, M. Zimine, G. Jung, I. H. M. van Stokkum, L. De Cola, R. M. Williams and F. Wurthner, *J. Am. Chem. Soc.*, 2005, **127**, 6719.
9 M. Barboiu, E. Petit, A. van der Lee and G. Vaughan, *Inorg. Chem.*, 2006, **45**, 484.
10 J. R. Price, Y. H. Lan, G. B. Jameson and S. Brooker, *Dalton Trans.*, 2006, 1491.
11 K. F. Cheng, N. A. Thai, L. C. Teague, K. Grohmann and C. M. Drain, *Chem. Commun.*, 2005, 4678.
12 S. Alam Mohammad, S. Stromsdorfer, V. Dremov, P. Muller, J. Kortus, M. Ruben and J.-M. Lehn, *Angew. Chem., Int. Ed.*, 2005, **44**, 7896.
13 O. Shoji, H. Tanaka, T. Kawai and Y. Kobuke, *J. Am. Chem. Soc.*, 2005, **127**, 8598.
14 J. E. Beves, B. E. Chapman, P. W. Kuchel, L. F. Lindoy, J. McMurtrie, M. McPartlin, P. Thordarson and G. Wei, *Dalton Trans.*, 2006, 744.

15 G. A. Timco, A. S. Batsanov, F. K. Larsen, C. A. Muryn, J. Overgaard, S. J. Teat and R. E. P. Winpenny, *Chem. Commun*., 2005, 3649.
16 M. Affronte, I. Casson, M. Evangelisti, A. Candini, S. Carretta, C. Muryn, S. J. Teat, G. A. Timco, W. Wernsdorfer and R. E. P. Winpenny, *Angew. Chem., Int. Ed*., 2005, **44**, 6496.
17 J. Jiao, G. J. Long, L. Rebbouh, F. Grandjean, A. M. Beatty and T. P. Fehlner, *J. Am. Chem. Soc*., 2005, **127**, 17819.
18 R. H. Laye, F. K. Larsen, J. Overgaard, C. A. Muryn, E. J. L. McInnes, E. Rentschler, V. Sanchez, S. J. Teat, H. U. Gudel, O. Waldmann, G. A. Timco and R. E. P. Winpenny, *Chem. Commun*., 2005, 1125.
19 Y. Lee, A. A. N. Sarjeant and K. D. Karlin, *Chem. Commun*., 2006, 621.
20 E. M. Rumberger, S. J. Shah, C. C. Beedle, L. N. Zakharov, A. L. Rheingold and D. N. Hendrickson, *Inorg. Chem*., 2005, **44**, 2742.
21 D. Foguet-Albiol, K. A. Abboud and G. Christou, *Chem. Commun*., 2005, 4282.
22 T. C. Stamatatos, S. Dionyssopoulou, G. Efthymiou, P. Kyritsis, C. P. Raptopoulou, A. Terzis, R. Vicente, A. Escuer and S. P. Perlepes, *Inorg. Chem*., 2005, **44**, 3374.
23 R. P. John, K. Lee, B. J. Kim, B. J. Suh, H. Rhee and M. S. Lah, *Inorg. Chem*., 2005, **44**, 7109.
24 A. A. Mohamed, A. Burini and J. P. Fackler, *J. Am. Chem. Soc*., 2005, **127**, 5012.
25 S.-Y. Yu, Z.-X. Zhang, E. C.-C. Cheng, Y.-Z. Li, V. W.-W. Yam, H.-P. Huang and R. Zhang, *J. Am. Chem. Soc*., 2005, **127**, 17994.
26 F. H. Fry, B. A. Dougan, N. McCann, C. J. Ziegler and N. E. Brasch, *Inorg. Chem*., 2005, **44**, 5197.
27 Z. Mao, J. S. Huang, C. M. Che, N. Y. Zhu, S. K. Y. Leung and Z. Y. Zhou, *J. Am. Chem. Soc*., 2005, **127**, 4562.
28 D. Dragancea, V. B. Arion, S. Shova, E. Rentschler and N. V. Gerbeleu, *Angew. Chem., Int. Ed*., 2005, **44**, 7938.
29 A. Oleksi, A. G. Blanco, R. Boer, I. Uson, J. Aymami, A. Rodger, M. J. Hannon and M. Coll, *Angew. Chem., Int. Ed*., 2006, **45**, 1227.
30 J. M. Senegas, S. Koeller, G. Bernardinelli and C. Piguet, *Chem. Commun*., 2005, 2235.
31 M. Albrecht, S. Dehn, G. Raahe and R. Frolich, *Chem. Commun*., 2005, 5690.
32 F. E. Hahn, T. Kreickmann and T. Pape, *Dalton Trans*., 2006, 769.
33 L. Natrajan, J. Pecaut and M. Mazzanti, *Dalton Trans*., 2006, 1002.
34 V. Baskar and P. W. Roesky, *Dalton Trans*., 2006, 676.
35 I. M. Muller, D. Moller and K. Focker, *Chem.–Eur. J*., 2005, **11**, 3318.
36 I. M. Muller and D. Moller, *Angew. Chem., Int. Ed*., 2005, **44**, 2969.
37 H. Amouri, L. Mimassi, M. N. Rager, B. E. Mann, C. Guyard-Duhayon and L. Raehm, *Angew. Chem., Int. Ed*., 2005, **44**, 4543.
38 S. P. Argent, T. Riis-Johannessen, J. C. Jeffery, L. P. Harding and M. D. Ward, *Chem. Commun*., 2005, 4647.
39 S. P. Argent, H. Adams, T. Riis-Johannessen, J. C. Jeffery, L. P. Harding, O. Mamula and M. D. Ward, *Inorg. Chem*., 2006, **45**, 3905.
40 S. P. Argent, H. Adams, T. Riis-Johannessen, J. C. Jeffery, L. P. Harding and M. D. Ward, *J. Am. Chem. Soc*., 2006, **128**, 72.
41 C. J. Sumby and M. L. Hardie, *Angew. Chem., Int. Ed*., 2005, **44**, 6395.
42 T. Haino, M. Kobayashi and Y. Fukazawa, *Chem.–Eur. J*., 2006, **12**, 3310.
43 M. Yamanaka, Y. Yamada, Y. Sei, K. Yamaguchi and K. Kobayashi, *J. Am. Chem. Soc*., 2006, **128**, 1531.
44 C. S. Campos-Fernandez, B. L. Schottel, H. T. Chifotides, J. K. Bera, J. Bacsa, J. M. Koomen, D. H. Russell and K. R. Dunbar, *J. Am. Chem. Soc*., 2005, **127**, 12909.
45 A. W. Kleij, M. Kuil, D. M. Tooke, M. Lutz, A. L. Spek and J. N. H. Reek, *Chem.–Eur. J*., 2005, **11**, 4743.
46 S. H. Li, H. P. Huang, S. Y. Yu, Y. Z. Li, H. Huang, Y. Sei and K. Yamaguchi, *Dalton Trans*., 2005, 2346.
47 D. Fiedler, R. G. Bergman and K. N. Raymond, *Angew. Chem., Int. Ed*., 2006, **45**, 745.
48 B. E. F. Tiedemann and K. N. Raymond, *Angew. Chem., Int. Ed*., 2006, **45**, 83.
49 A. V. Davis and K. N. Raymond, *J. Am. Chem. Soc*., 2005, **127**, 7912.
50 R. M. Yeh, J. Xu, G. Seeber and K. N. Raymond, *Inorg. Chem*., 2005, **44**, 6228.
51 F. A. Cotton, C. A. Murillo and R. Yu, *Dalton Trans*., 2005, 3161.
52 M. Tominaga, K. Suzuki, T. Murase and M. Fujita, *J. Am. Chem. Soc*., 2005, **127**, 11950.
53 K. Takaoka, M. Kawano, T. Ozeki and M. Fujita, *Chem. Commun*., 2006, 1625.
54 M. Yoshizawa, T. Kusukawa, M. Kawano, T. Ohhara, I. Tanaka, K. Kurihara, N. Niimura and M. Fujita, *J. Am. Chem. Soc*., 2005, **127**, 2798.
55 S. Tashiro, M. Tominaga, Y. Yamaguchi, K. Kato and M. Fujita, *Chem.–Eur. J*., 2006, **12**, 3211.

56 M. Kawano, Y. Kobayashi, T. Ozeki and M. Fujita, *J. Am. Chem. Soc.*, 2006, **128**, 6558.
57 M. Yoshizawa, K. Kumazawa and M. Fujita, *J. Am. Chem. Soc.*, 2005, **127**, 13456.
58 M. Yoshizawa, J. Nakagawa, K. Kurnazawa, M. Nagao, M. Kawano, T. Ozeki and M. Fujita, *Angew. Chem., Int. Ed.*, 2005, **44**, 1810.
59 M. Yoshizawa, K. Ono, K. Kumazawa, T. Kato and M. Fujita, *J. Am. Chem. Soc.*, 2005, **127**, 10800.
60 Z. Ni, A. Yassar, T. Antoun and O. M. Yaghi, *J. Am. Chem. Soc.*, 2005, **127**, 12752.
61 D. Moon, S. Kang, J. Park, K. Lee, R. P. John, H. Won, G. H. Seong, Y. S. Kim, G. H. Kim, H. Rhee and M. S. Lah, *J. Am. Chem. Soc.*, 2006, **128**, 3530.
62 P. de Wolf, P. Waywell, M. Hanson, S. L. Heath, A. J. H. M. Meijer, S. J. Teat and J. A. Thomas, *Chem.–Eur. J.*, 2006, **12**, 2188.
63 C. E. Dube, S. Mukhopadhyay, P. J. Bonitatebus, R. J. Staples and W. H. Armstrong, *Inorg. Chem.*, 2005, **44**, 5161.
64 H. C. Yao, Y. Z. Li, Y. Song, Y. S. Ma, L. M. Zheng and X. Q. Xin, *Inorg. Chem.*, 2006, **45**, 59.
65 P. King, W. Wernsdorfer, K. A. Abboud and G. Christou, *Inorg. Chem.*, 2005, **44**, 8659.
66 R. T. W. Scott, S. Parsons, M. Murugesu, W. Wernsdorfer, G. Christou and E. K. Brechin, *Angew. Chem., Int. Ed.*, 2005, **44**, 6540.
67 S. Piligkos, G. Rajaraman, M. Soler, N. Kirchner, J. van Slageren, R. Bircher, S. Parsons, H. U. Gudel, J. Kortus, W. Wernsdorfer, G. Christou and E. K. Brechin, *J. Am. Chem. Soc.*, 2005, **127**, 5572.
68 S. Tanase, G. Aromi, E. Bouwman, H. Kooijman, A. L. Spek and J. Reedijk, *Chem. Commun.*, 2005, 3147.
69 C. M. Zaleski, E. C. Depperman, C. Dendrinou-Samara, M. Alexiou, J. W. Kampf, D. P. Kessissoglou, M. L. Kirk and V. L. Pecoraro, *J. Am. Chem. Soc.*, 2005, **127**, 12862.
70 H. Oshio, M. Nihei, S. Koizumi, T. Shiga, H. Nojiri, M. Nakano, N. Shirakawa and M. Akatsu, *J. Am. Chem. Soc.*, 2005, **127**, 4568.
71 D. Li, S. Parkin, G. Wang, G. T. Yee, R. Clerac, W. Wernsdorfer and S. M. Holmes, *J. Am. Chem. Soc.*, 2006, **128**, 4214.
72 S. J. Langley, M. Helliwell, R. Sessoli, P. Rosa, W. Wernsdorfer and R. E. P. Winpenny, *Chem. Commun.*, 2005, 5029.
73 S. Akine, T. Matsumoto, T. Taniguchi and T. Nabeshima, *Inorg. Chem.*, 2005, **44**, 3270.
74 M. Nihei, M. Ui, M. Yokota, L. Q. Han, A. Maeda, H. Kishida, H. Okamoto and H. Oshio, *Angew. Chem., Int. Ed.*, 2005, **44**, 6484.
75 W. Saalfrank Rolf, C. Schmidt, H. Maid, F. Hampel, W. Bauer and A. Scheurer, *Angew. Chem., Int. Ed.*, 2005, **45**, 315.
76 A. K. Boudalis, C. P. Raptopoulou, B. Abarca, R. Ballesteros, M. Chadlaoui, J.-P. Tuchagues and A. Terzis, *Angew. Chem., Int. Ed.*, 2006, **45**, 432.
77 A. Bell, G. Aromi, S. J. Teat, W. Wernsdorfer and R. E. P. Winpenny, *Chem. Commun.*, 2005, 2808.
78 X. K. Fang, T. M. Anderson and C. L. Hill, *Angew. Chem., Int. Ed.*, 2005, **44**, 3540.
79 D. L. Long, H. Abbas, P. Kogerler and L. Cronin, *Angew. Chem., Int. Ed.*, 2005, **44**, 3415.
80 T. M. Anderson, R. Cao, E. Slonkina, B. Hedman, K. O. Hodgson, K. I. Hardcastle, W. A. Neiwert, S. X. Wu, M. L. Kirk, S. Knottenbelt, E. C. Depperman, B. Keita, L. Nadjo, D. G. Musaev, K. Morokuma and C. L. Hill, *J. Am. Chem. Soc.*, 2005, **127**, 11948.
81 B. Godin, Y. G. Chen, J. Vaissermann, L. Ruhlmann, M. Verdaguer and P. Gouzerh, *Angew. Chem., Int. Ed.*, 2005, **44**, 3072.
82 N. Belai and M. T. Pope, *Chem. Commun.*, 2005, 5760.
83 B. Godin, J. Vaissermann, P. Herson, L. Ruhlmann, M. Verdaguer and P. Gouzerh, *Chem. Commun.*, 2005, 5624.
84 B. S. Bassil, S. Nellutla, U. Kortz, A. C. Stowe, J. van Tol, N. S. Dalal, B. Keita and L. Nadjo, *Inorg. Chem.*, 2005, **44**, 2659.
85 J. M. Clemente-Juan, E. Coronado, A. Gaita-Arino, C. Gimenez-Saiz, H. U. Gudel, A. Sieber, R. Bircher and H. Mutka, *Inorg. Chem.*, 2005, **44**, 3389.